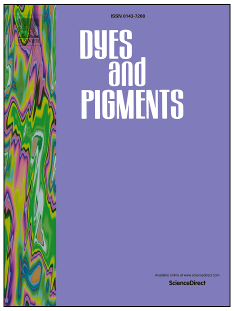

Synthesis and characterization of amphiphilic silica nanoparticles covered by block copolymers branching photochromic diarylethene moieties on side chain

Ryuta Seno , Seiya Kobatake

PII: S0143-7208(14)00440-9
DOI: 10.1016/j.dyepig.2014.11.010
Reference: DYPI 4588

To appear in: *Dyes and Pigments*

Received Date: 15 September 2014
Revised Date: 6 November 2014
Accepted Date: 10 November 2014

Please cite this article as: Seno R, Kobatake S, Synthesis and characterization of amphiphilic silica nanoparticles covered by block copolymers branching photochromic diarylethene moieties on side chain, *Dyes and Pigments* (2014), doi: 10.1016/j.dyepig.2014.11.010.

Revised Manuscript for publication in *Dyes and Pigments*

Synthesis and characterization of amphiphilic silica nanoparticles covered by block copolymers branching photochromic diarylethene moieties on side chain

Ryuta Seno and Seiya Kobatake*

Department of Applied Chemistry, Graduate School of Engineering, Osaka City University, 3-3-138 Sugimoto, Sumiyoshi-ku, Osaka 558-8585, Japan

Corresponding author. Tel./fax: +81 6 6605 2797.
E-mail address: kobatake@a-chem.eng.osaka-cu.ac.jp (S. Kobatake).

ABSTRACT

Silica nanoparticles covered with polystyrene branching diarylethene moieties to the side chains are synthesized by reversible addition-fragmentation chain transfer polymerization on silica nanoparticles. The resulting nanoparticles are soluble in toluene and tetrahydrofuran and show reversible photoisomerization upon alternating irradiation with ultraviolet and visible light. The photoreversible isomerization follows color change, which is called photochromism. During the photochromic reactions, the nanoparticles are dispersed in solutions such as terahydrofuran. The modification by further block copolymerization of *N*-isopropylacrylamide results in fabrication of photochromic silica nanoparticles soluble in both tetrahydrofuran and water.

Keywords: Silica nanoparticle; RAFT polymerization; Photochromism; Diarylethene; Sedimentation

1. Introduction

Inorganic nanoparticles covered with organic polymers have drawn much attention as organic/inorganic hybrid materials in recent years because of their applications for optical materials, paints, makeup, column fillers, and solar cells [1-4]. Inorganic silica nanoparticles have characteristics such as simple fabrications of controlled particular size, low cost, weather resistance, chemical resistance, and safeness. Silica nanoparticles covered with the functional dyes is useful as novel functional dyes and pigments which have the potential for toughness and durability. The various types of fluorescent dyes attached on silica nanoparticles have recently been used for reversible fluorescence switch for biological imaging [5-10]. The fluorescence modulation is based on a photochromic molecular switch incorporated into the silica nanoparticles. The biocompatibility of the silica nanoparticles makes promising materials for in vivo imaging applications. Such organic/inorganic hybrid materials can improve the solubility in solvents by the modification of the covering agents.

Photochromic compounds exhibit reversible transformations between two isomers upon irradiation at an appropriate wavelength of light [11,12]. The interconversion between the two states is accompanied by changes in the physical properties such as absorption spectra, fluorescence, refractive indices, dielectric constants, oxidation–reduction potentials, and so on. Diarylethene is one of typical P-type photochromic compounds and shows reversible photoisomerization upon alternating irradiation with ultraviolet (UV) and visible light [13-16]. Silica nanoparticles with diarylethene polymers are expected to be used for application as a photochromic pigment having toughness and durability because of high dispersibility of the particle in organic solvents in addition to thermal stability and fatigue-resistant properties. Photochromic hybrid materials can be applied as photochromic decoloration, photochromic glasses, UV sensors, photochromic optical waveguide, optical memorydevices, holographic recording media, non-linear optics, and so on [17].

The “grafting-from” and “grafting-to” techniques in polymer chemistry are commonly used for connecting polymer chains on solid substrate [18-20]. Among them, the former method can connect polymer with functional group on substrate, whereas the latter method can initiate polymerization from substrate on which an initiator or a chain transfer agent presents to form grafting polymer chains in high density. Particularly, living radical polymerizations on the surface of materials are widely used for grafting on substrate because of easy control of polymer chain length and end groups. There are some reports on the surface-initiated living radical polymerizations such as atom transfer radical polymerization and reversible addition-fragmentation chain transfer (RAFT) polymerization [21,22]. Tsujii and coworkers found that high-density polymer brushes can be obtained by living radical polymerization from solid substrate [21]. Moreover, they demonstrated that the dispersibility of silica nanoparticles covered with polymer brushes in organic solvents is dominated by the nature of the polymers fabricated onto the silica nanoparticles [23].

Here, we report on fabrication of silica nanoparticles covered with polystyrene having photochromic diarylethene chromophores to the side chains, as shown in Scheme 1. The silica surface-initiated polymerization was carried out by RAFT copolymerization of styrene (St) and a diarylethene monomer (DE) using silica nanoparticle covered with a RAFT agent. To modify the solubility of the nanoparticles in both hydrophobic and hydrophilic solvents, block copolymerization with *N*-isopropylacrylamide (NIPAm) was also performed. The photochromic behavior and dispersibility of the resulting nanoparticles in THF and water are discussed.

[Scheme 1]

2. Experimental section

2.1. Measurements

^{1}H NMR spectra were measured using a Bruker AV-300N NMR spectrometer at 300 MHz. Deuterated chloroform ($CDCl_3$) was used as the solvent and tetramethylsilane (TMS) as internal standard, respectively. Transmission electron microscopy (TEM; Hitachi H-7000) was performed at an accelerating voltage of 75 kV. TEM samples were prepared by dropping an ethanol or tetrahydrofuran (THF) solution of the particles on a carbon-coated copper grid and dried in air. The particle size was determined from the TEM image. Absorption spectra were measured using a UV/visible absorption spectrophotometer (Jasco V-560). Photoirradiation was conducted using a 200 W mercury-xenon lamp (Moritex MUV-202) or a 300 W xenon lamp (Asahi Spectra MAX-301) as a light source. Monochromatic light was obtained by passing the light through a monochromator (Jobin Yvon H10 UV or Jasco CT-10) and glass filters. Gel-permeation chromatography (GPC) was performed using a Tosoh 8000 series GPC system equipped with TSK-gel columns at 40 °C and using THF as the eluent.

2.2. Materials

All reagents were purchased from Wako Pure Chemical Industries. NIPAm and 2,2’-azobis(2,4,4-trimethylpentane) (ATMP) were recrystallized from *n*-hexane. DE was synthesized according to the method described in our previous paper [24].

2.3. Synthesis of 1-[3-(methoxydimethylsilyl)propyloxycarbonyl]ethyl dithiobenzoate (RAFT-Si)

RAFT-Si was synthesized according to the method described in literature as follows [25]. Phenylmagnesium bromide was prepared from bromobenzene (12.4 mL, 118 mmol) and magnesium turnings (1.90 g, 78.2 mmol) in dry THF (30 mL). Carbon disulfide (4.80 mL, 79.5 mmol) was slowly added to the THF solution of the Grignard reagent at 40 °C. To the mixture was slowly added 3-(methoxydimethylsilyl)propyl 2-bromopropionate (20.2 g, 71.2 mmol) at 40 °C. The mixture was stirred for 24 h at room temperature. An adequate amount of ice water was added to the mixture to quench the reaction. The reaction mixture was extracted with ether, washed with brine, dried over $MgSO_4$, filtrated, and concentrated in vacuo. The crude product was purified by column chromatography on silica gel using *n*-hexane/ethyl acetate (8:2) as the eluent. The pure product was obtained by a recycle HPLC (JAI LC-908) on gel columns (JAIGEL-1H and 2H) using $CHCl_3$ as the eluent in 72.2% yield (18.3 g). ^{1}H NMR (300 MHz, $CDCl_3$, TMS): δ (ppm) = 0.11 (s, 6H, $Si(C\underline{H}_3)_2OCH_3$), 0.56-0.65 (m, 2H, $COOCH_2CH_2C\underline{H}_2$), 1.67-1.75 (m, 2H, $COOCH_2C\underline{H}_2$), 1.68 (d, J = 7.4 Hz, 3H, $SCHC\underline{H}_3CO$), 3.41 (s, 3H, $Si(CH_3)_2OC\underline{H}_3$), 4.09-4.17 (m, 2H, $COOC\underline{H}_2$), 4.75 (q, J = 7.4 Hz, 1H, $SC\underline{H}CH_3CO$), 7.26-7.57 (m, 3H, Aromatic H), 7.97-8.01 (m, 2H, Aromatic H).

2.4. Synthesis of 1-(ethoxycarbonyl)ethyl dithiobenzoate (EEDB)

EEDB was synthesized according to the method described in literature as follows [26]. Phenylmagnesium bromide was prepared from bromobenzene (10.5 mL, 100 mmol) in THF (50 mL) and magnesium turnings (2.43 g, 100 mmol) in dry THF (7 mL) by heating for 20 min at 60 °C. Carbon disulfide (6.10 mL, 101 mmol) was slowly added to the THF solution of the Grignard reagent at 40-50 °C. To the mixture was slowly added ethyl 2-bromopropionate (18.1 g, 100 mmol) at 40 °C. The mixture was stirred for 16 h at room temperature. An adequate amount of ice water was added to the mixture to quench the reaction. The reaction mixture was extracted with ether, washed with brine, dried over $MgSO_4$, filtrated, and concentrated in vacuo. The crude product was purified by column chromatography on silica gel using *n*-hexane as the eluent. The pure product was obtained by a recycle HPLC (JAI LC-908) on gel columns (JAIGEL-1H and 2H) using $CHCl_3$ as the eluent in 37.8% yield (9.62 g). ^{1}H NMR (300

MHz, $CDCl_3$, TMS): δ = 1.29 (t, J = 7.1 Hz, 3H, CH_2CH_3), 1.67 (d, J = 7.4 Hz, 3H, $CHCH_3$), 4.23 (q, J = 7.1 Hz, 2H, CH_2), 4.75 (q, J = 7.4 Hz, 1H, CH), 7.34-7.43 (m, 2H, Aromatic H), 7.51-7.58 (m, 1H, Aromatic H), 7.95-8.03 (m, 2H, Aromatic H).

2.5. Synthesis of silica nanoparticle by the Stöber method

A 28 wt% aqueous solution of ammonia and absolute ethanol (50 mL) were added into a flask. To the solution was added a solution of tetraethoxysilane (TEOS) and absolute ethanol (50 mL). The mixture was stirred for 24 h at room temperature. Silica nanoparticles were obtained as solid by centrifuging for 10 min at 6000 rpm in ethanol. The silica nanoparticles were purified by centrifuging 5 times in ethanol. The silica nanoparticles obtained were dried in vacuo.

2.6. Synthesis of silica nanoparticle covered with RAFT agent

The silica nanoparticles obtained above were added to 2 N hydrochloric acid, and the mixture was stirred for 24 h at room temperature. The silica nanoparticles were washed by distilled water and purified by centrifuging 5 times in distilled water, and dried. The silica nanoparticles were added to a dry THF solution (10 mL) of RAFT-Si (500 mg, 1.4 mmol). The mixture was refluxed for 18 h. The resulting silica nanoparticles were purified by centrifuging 5 times in *n*-hexane. The nanoparticles (SNP-RAFT) were dried in vacuo.

2.7. Polymerization

RAFT polymerization was carried out in a glass tube sealed under vacuum. Monomer, EEDB, SNP-RAFT, ATMP, and toluene were put in a glass tube. The tube was degassed by several freeze-pump-thaw cycles and sealed off under vacuum. After polymerization for a prescribed time at 100 °C, the resulting nanoparticles were collected as solid by centrifugation for 10 min at 6000 rpm and washed 5 times with

THF followed by drying in vacuo. The silica-free polymer was collected by precipitation in methanol.

2.8. *Block copolymerization*

NIPAm, EEDB, AIBN, *N*,*N*-dimethylformamide (DMF), and SNP-poly(St-*co*-DE) were put in a glass tube. The tube was degassed by several freeze-pump-thaw cycles and sealed off under vacuum. After polymerization for a prescribed time at 60 °C, the resulting nanoparticles were collected as solid by centrifugation for 10 min at 6000 rpm and washed 5 times in THF followed by drying in vacuo. The silica-free poly(NIPAm) was isolated by precipitation in *n*-hexane.

2.9. *Sedimentaion behavior*

The sedimentation behavior of the nanoparticles in solution was observed by the light-transmission method of the nanoparticles in THF and in water. Before the measurement, the solution of the nanoparticles was irradiated with 313 nm light to reach the photostationary state. The number of the nanoparticles in solution was determined from absorbance of the diarylethene closed-ring form at absorption maximum wavelength in the visible region.

3. Results and Discussion

3.1. Synthesis of RAFT-SNP

Silica nanoparticles were synthesized according to the technique established by Stöber and coworkers [27]. The Stöber method has characteristic to produce a monodispersed silica nanoparticle with small size distribution. The diameter of the particle is controlled by adjusting the concentrations of TEOS, water, and ammonia. Table 1 shows the preparation conditions and the properties of the resulting silica nanoparticles. The reaction was performed by stirring the solution of TEOS, water, and ammonia in ethanol for 24 h at room temperature under argon atmosphere, and the resulting silica nanoparticles were isolated and purified by centrifuging the suspension in ethanol. After drying the resulting silica nanoparticles, they were distributed in ethanol, and casted on the copper grid to measure TEM. The average particle diameter (d) and the standard deviation (σ) were obtained from the TEM image. Figure 1 shows the TEM images of the resulting silica nanoparticles. The silica nanoparticles have particle diameters of 60-350 nm and narrow particle size distributions (σ/d = 5-10%). The relationship between the d value and the concentration of ammonia used for the reaction was plotted in Figure 2. The d value can be controlled by the concentration of ammonia because the particle size increased with increasing the concentration of ammonia.

[Table 1]

[Figure 1]

[Figure 2]

The RAFT agent, RAFT-Si, is required to be immobilized onto the silica nanoparticle surface. In general, the silane coupling agent with a methoxysilyl group to attach the silica nanoparticle surface is used under the basic condition. Because the

RAFT agent is unstable under the basic condition, it is necessary to use the immobilization technique of the silane coupling agent without the basic condition. Thus, the silica nanoparticles were treated with hydrochloric acid and washed with distilled water, followed by refluxing the THF solution of RAFT-Si under argon atmosphere. The siloxane bond was formed by the reaction of the ethoxysilyl group of RAFT-Si and the silanol group on the silica nanoparticle surface. The resulting SNP-RAFT has a pale red color originated from dithiobenzoate group. This means that the RAFT agent is successfully immobilized onto the silica nanoparticle.

3.2. Synthesis and characterization of SNP-poly(St-co-DE)

RAFT copolymerization of DE and St using SNP-RAFT as the RAFT agent was carried out at 100 °C. The RAFT polymerization using SNP-RAFT without a silica-free RAFT agent cannot control M_n and M_w/M_n of the grafting polymers [22]. Therefore, EEDB as the silica-free RAFT agent was added to the polymerization mixture. Table 2 shows the polymerization condition and the results of the polymerization. Two different sizes of SNP were used for the polymerization. After the polymerization, SNP-poly(St-*co*-DE) was collected as solid by centrifugation, and silica-free poly(St-*co*-DE) was isolated by precipitation to methanol. Figure 3 shows TEM images of SNP-poly(St-*co*-DE). The silica core maintains particle diameter and narrow particle size distribution. The polymer shell around the silica core is observed in the image. The thickness of the polymer shell in dry was found to be 3-6 nm from the image. This means that RAFT polymerization was successfully carried out to form SNP-poly(St-*co*-DE).

[Table 2]

[Figure 3]

The composition of DE in silica-free poly(St-*co*-DE) was determined to be 34-39 mol% by ^{1}H NMR spectroscopy, whereas the composition of DE in monomer is 25 mol%. The copolymer has a M_n of 17000-30000 and a low polydispersity (M_w/M_n = 1.1-1.2) determined by standard poly(St) calibration using GPC. The copolymer attached to the silica nanoparticle surface is considered to have the similar characteristics.

3.3. Photochromism of SNP-poly(St-co-DE)

Photochromic reaction behavior of SNP-poly(St-*co*-DE) was examined in THF and in neat powder. Figure 4 shows color change in SNP_{60}-poly(St-*co*-DE) with a diameter of SNP in 60 nm upon alternating irradiation with UV and visible light. The THF solution of the silica nanoparticle, which is well-dispersed in THF, turned blue by irradiation with UV light. The color was thermally stable and was bleached by irradiation with visible light. The powder of SNP-poly(St-*co*-DE) also shows blue color upon irradiation with UV light. The color was bleached by irradiation with visible light. The coloration and decoloration can be repeated several times. Figure 5 shows absorption spectral changes of poly(St-*co*-DE) and SNP-poly(St-*co*-DE) in THF upon alternating irradiation with UV and visible light. The open-ring form is colorless in THF. Upon irradiation with 313 nm light, new absorption band appeared at 450-700 nm, and the absorption band disappeared upon irradiation with visible light. The light scattering of the silica nanoparticles was observed in the measurement as an increase in the base line in Figure 5b. No change of the light scattering was observed during the photochromic reactions. SNP-poly(St-*co*-DE) was found to exhibit photochromism as well as poly(St-*co*-DE).

[Figure 4]

[Figure 5]

Figure 6 shows the photocyclization and photocycloreversion reactivities of SNP-poly(St-*co*-DE) and poly(St-*co*-DE) in THF upon irradiation with 313 nm light and 600 nm light, respectively. There is no difference in the photocyclization and photocycloreversion rates of DE for SNP-poly(St-*co*-DE) and poly(St-*co*-DE); thus, the photoisomerization of DE takes place in high efficiency even in SNP-poly(St-*co*-DE). A few retardation on photocyclization and photocycloreversion reaction rates of SNP-poly(St-*co*-DE) is considered to be brought by light scattering of the silica nanoparticles.

[Figure 6]

3.4. Synthesis and characterization of amphiphilic photochromic silica nanoparticles

Block copolymerization of NIPAm using SNP-poly(St-*co*-DE) was carried out in DMF using AIBN as the initiator at 60 °C. Table 3 shows the polymerization conditions and the results of the polymerization. The polymerization was successfully carried out in a glass tube for 20 h or 40 h at 60 °C. Figure 7 shows TEM images of SNP-poly(St-*co*-DE)-*block*-poly(NIPAm). The TEM images show that the particles were well-dispersed in THF and spread on the copper grid without aggregation. The polymer layer was also observed in the vicinity of the silica nanoparticles with the layer thickness of 5-10 nm.

[Table 3]

[Figure 7]

The degree of polymerization for poly(NIPAm) segment in poly(St-*co*-DE)-*block*-poly(NIPAm) can be determined from the ^{1}H-NMR spectrum of silica-free poly(NIPAm) obtained simultaneously by the polymerization. Figure 8 shows ^{1}H-NMR spectrum of poly(NIPAm). The broad peak at 0.4-2.7 ppm is assigned to the methylene and methine protons in the main chain of the polymer. The peaks at 1.14 and 3.8-4.4 ppm are assigned to methyl and methine protons of isopropyl group, respectively. The broad peak at 5.5-7.7 ppm is due to the NH proton. The aromatic protons of the dithiobenzoate group at the polymer end appeared at 7.39, 7.56, and 7.96 ppm. The degree of polymerization of poly(NIPAm) was determined base on the comparison of the proton intensities of the aromatic protons at the polymer end and the methine protons of the isopropyl group in the monomer unit. The results are shown in Table 3.

[Figure 8]

3.5. *Photochromism of SNP-poly(St-co-DE)-block-poly(NIPAm)*

The resulting SNP-poly(St-*co*-DE)-*block*-poly(NIPAm) is soluble in THF and water. The photochromic behavior of the nanoparticles was examined in THF and water upon alternating irradiation with UV and visible light. Figure 9 shows absorption spectral changes of the nanoparticles in THF and water. Upon irradiation with UV light, the solution turned blue both in THF and water. The absorption maximum wavelength in the visible region appeared at 622 and 613 nm in THF and water, respectively. The maximum wavelength of silica-free poly(DE) and SNP-poly(St-*co*-DE) in THF is 592 nm. Therefore, the red shift of 30 nm is ascribed to the presence of the poly(NIPAm) segment. Although the poly(NIPAm) segment is introduced to the polymer chain as a block segment, it is considered to affect an absorption property of diarylethene in THF and water. The pendant diarylethene chromophore in poly(St-*co*-DE) is considered to serve as surrounded by hydrophilic poly(NIPAm). Therefore, the shift is due to the local structure around the diarylethene chromophore. The instability of diarylethene molecule at the ground state brings about the red shift of the absorption spectrum of the closed-ring form.

[Figure 9]

3.6. Dispersibility of SNP-poly(St-co-DE)-block-poly(NIPAm) in solution

The hydrophilicity of the silica nanoparticle covered with the diarylethene chromophore can be expected to improve by introducing the poly(NIPAm) segment into the outside of SNP-poly(St-*co*-DE) by block copolymerization. The dispersibility of SNP_{60}-poly(St-*co*-DE) and SNP_{60}-poly(St-*co*-DE)-*block*-poly(NIPAm) in THF and water was observed by the sedimentation behavior of the particles, as shown in Figure 10. In THF, both nanoparticles are well-dispersed. However, in water, SNP_{60}-poly(St-*co*-DE) was not dispersed because of the hydrophobic polymer chain. On the other hand, SNP_{60}-poly(St-*co*-DE)-*block*-poly(NIPAm) was well-distributed in water as well as in THF.

[Figure 10]

The chain length dependence of poly(NIPAm) segment on dispersibility in water was examined. Figure 11 shows the time dependence of the number of SNP_{60}-poly(St-*co*-DE)-*block*-poly(NIPAm) (m = 137) and SNP_{60}-poly(St-*co*-DE)-*block*-poly(NIPAm) (m = 217). The polymer chain length of the latter particles is 1.5 times longer than that of the former particle. Both of the nanoparticles were dispersed highly in water and 88% of particles maintain a dispersion state even after 2 h. This means that the poly(NIPAm) segment is long enough to disperse in water.

[Figure 11]

Poly(NIPAm) shows lower critical solution temperature (LCST) near room temperature. Therefore, the sedimentation behavior of SNP$_{60}$-poly(St-*co*-DE)-*block*-poly(NIPAm) was examined at 25 and 40 °C, as shown in Figure 12. The sedimentation speed of the particles was estimated from the slope of the linear relationship to be 1.1×10^{11} and 1.4×10^{11} particles L^{-1} min^{-1} at 25 and 40 °C, respectively. The speed at 40 °C is 1.3 times faster than that at 25 °C. Although this is due to the decrease in the hydrophilicity of the poly(NIPAm) segment at 40 °C, the large difference of the sedimentation behavior was not observed. It is concluded that SNP-poly(St-*co*-DE)-*block*-poly(NIPAm) is well-dispersed in water even at a temperature above LCST.

[Figure 12]

4. Conclusion

We succeeded in preparing a novel photochromic pigment that originates from silica nanoparticles and photochromic polymers. The photochromic silica nanoparticles showed photochromism in high efficiency in solution and neat powder. According to introduction of the poly(NIPAm) segment by the block copolymerization, the silica nanoparticles were well-dispersed in both THF and water. Such amphiphilic silica nanoparticles covered with photochromic diarylethene chromophores can be useful for applications such as organic/inorganic hybrid photochromic pigments.

Acknowledgments

This work was partly supported by a Grant-in-Aid for Scientific Research (C) (No. 24550161) from the Japan Society for the Promotion of Science (JSPS) and a Grant-in-Aid for Scientific Research on Innovative Areas "Photosynergetics" (No. 26107013) from MEXT, Japan.

References

[1] Huynh WU, Dittmer JJ, Alivisatos AP. Hybrid nanorod-polymer solar cells. Science 2002; 295: 2425–7.

[2] Sanchez C, Julián B, Belleville P, Popall M. Applications of hybrid organic–inorganic nanocomposites. J Mater Chem 2005; 15: 3559–92.

[3] Nagase K, Kobayashi J, Kikuchi A., Akiyama Y, Kanazawa H, Okano T. Thermoresponsive polymer brush surfaces with hydrophobic groups for all-aqueous chromatography. ACS Appl Mater Interfaces 2012; 4: 1998–2008.

[4] Plass R, Pelet S, Krueger J, Grätzel M. Quantum dot sensitization of organic–inorganic hybrid solar cells. J Phys Chem B 2002; 106: 7578–80.

[5] Fölling J, Polyakova S, Belov V, van Blaaderen A, Bossi ML, Hell SW. Synthesis and characterization of photoswitchable fluorescent silica nanoparticles. Small 2008; 4: 134–142.

[6] Zhao X, Bagwe RP, Tan W. Development of organic-dye-doped silica nanoparticles in a reverse microemulsion. Adv Mater 2004; 16: 173–6.

[7] Tran HN, Nghiem THL, Vu TTD, Pham MT, Nguyen TV, Tran TT, et al. Dye-doped silica-based nanoparticles for bioapplications. Adv Nat Sci: Nanosci Nanotechnol 2013; 4: 043001.

[8] Bae SW, Tan W, Hong J-I. Fluorescent dye-doped silica nanoparticles: new tools for bioapplications. Chem Commun 2012; 48: 2270–82.

[9] Jung H, You S, Lee C, You S, Kim Y. One-pot synthesis of monodispersed silica nanoparticles for diarylethene-based reversible fluorescence photoswitching in living cells. Chem Commun 2013; 49: 7528–30.

[10] Pedone A, Prampolini G, Monti S, Barone V. Realistic modeling of fluorescent dye-doped silica nanoparticles: a step toward the understanding of their enhanced photophysical properties. Chem Mater 2011; 23: 5016–23.

[11] Brown GH. Photochromism, Wiley-Interscience, New York, 1971.

[12] Dürr H, Bouas-Laurent H. Photochromism: Molecules and Systems, Elsevier, Amsterdam, 2003.

[13] Irie M. Diarylethenes for memories and switches. Chem Rev 2000; 100: 1685–716.

[14] Kobatake S, Irie M. Single-crystalline photochromism of diarylethenes. Bull Chem Soc Jpn 2004; 77: 195–210.

[15] Myles A J, Branda NR. 1,2-Dithienylethene photochromes and non-destructive erasable memory. Adv Funct Mater 2002; 12: 167–73.

[16] Tian H, Wang S. Photochromic bisthienylethene as multi-function switches. Chem Commun 2007: 781–92.

[17] Pardo R, Zayat M, Levy D. Photochromic organic-inorganic hybrid materials. Chem Soc Rev 2011; 40: 672–87.

[18] Milner ST. Polymer brushes. Science 1991; 251: 905–14.

[19] Zhao B, Brittain WJ. Polymer brushes: surface-immobilized macromolecules. Prog Polym Sci 2000; 25: 677–710.

[20] Minko S. Grafting on solid surfaces: “grafting to” and “grafting from” methods. In: Stamm M, editor. Polymer surfaces and interfaces: characterization, modification and applications, Berlin Heidelberg: Springer; 2008, p. 215–34 .

[21] Ejaz M, Yamamoto S, Ohno K, Tsujii Y, Fukuda T. Controlled graft polymerization of methyl methacrylate on silicon substrate by the combined use of the langmuir-blodgett and atom transfer radical polymerization techniques. Macromolecules 1998; 31: 5934–6.

[22] Tsujii Y, Ejaz M, Sato K, Goto A, Fukuda T. Mechanism and kinetics of RAFT-mediated graft polymerization of styrene on a solid surface. 1. Experimental evidence of surface radical migration. Macromolecules 2001; 34: 8872–8.

[23] Ohno K, Morinaga T, Koh K, Tsujii Y, Fukuda T. Synthesis of monodisperse silica particles coated with well-defined, high-density polymer brushes by surface-initiated atom transfer radical polymerization. Macromolecules 2005; 38: 2137–42.

[24] Kuratani H, Kobatake S. Photochromism of diarylethene-functionalized polystyrene with high conversion in a solid-state polymer film. Chem Lett 2006; 35: 628–9.

[25] Li C, Benicewicz BC. Synthesis of well-defined polymer brushes grafted onto silica nanoparticles via surface reversible addition–fragmentation chain transfer polymerization. Macromolecules 2005; 38: 5929–36.

[26] Farmer SC, Patten TE. (Thiocarbonyl-α-thio)carboxylic acid derivatives as transfer agents in reversible addition–fragmentation chain-transfer polymerizations. J Polym Sci Part A: Polym Chem 2002; 40: 555–63.

[27] Stöber W, Fink A, Bohn E. Controlled growth of monodisperse silica spheres in the micron size range. J Colloid Interf Sci 1968; 26: 62–9.

Figure Caption

Scheme 1. Synthetic scheme of an amphiphilic photochromic silica nanoparticle.

Figure 1. TEM images (left) and histograms of diameter distribution (right) for silica nanoparticles prepared by the Stöber method: [TEOS] = 0.11 mol L^{-1}, [NH_3] = 2.0 (a), 1.3 (b), 1.0 (c), 0.77 mol L^{-1} (d), [H_2O] = 2.4×[NH_3].

Figure 2. Relationship between the particle diameter of the silica nanoparticle and the concentration of ammonia used for the reaction. An error bar expresses the standard deviation of the particle diameter.

Figure 3. TEM images of SNP_{150}-poly(St-*co*-DE) (d = 150 nm, M_n = 27500) (a) and SNP_{60}-poly(St-*co*-DE) (d = 60 nm, M_n = 29800) (b).

Figure 4. Photographs of SNP_{60}-poly(St-*co*-DE) (M_n = 29800) before (left) and after (right) irradiation with UV light in THF (a) and neat powder (b).

Figure 5. Absorption spectral changes of poly(St-*co*-DE) (a) and SNP_{60}-poly(St-*co*-DE) (M_n = 29800) (b) in THF: open-ring form (- - -) and the photostationary state upon irradiation with 313 nm light (——).

Figure 6. Time-conversion plot of SNP_{60}-poly(St-*co*-DE) (M_n = 29800) (●) and poly(St-*co*-DE) (○) in photocyclization by irradiation with 313 nm light (a) and in photocycloreversion by irradiation with 600 nm light (b).

Figure 7. TEM images of SNP$_{150}$-poly(St-*co*-DE)-*block*-poly(NIPAm) (m = 160) (a) and SNP$_{60}$-poly(St-*co*-DE)-*block*-poly(NIPAm) (m = 137) (b).

Figure 8. ^{1}H NMR spectrum of silica-free poly(NIPAm) obtained by RAFT polymerization of NIPAm with SNP$_{150}$-poly(St-*co*-DE) in DMF for 20 h at 60 °C: [NIPAm] = 3.5 mol L^{-1}, [EEDB] = 16 mmol L^{-1}, [SNP$_{150}$-poly(St-*co*-DE)] = 10 g L^{-1}, [AIBN] = 8.0 mmol L^{-1}.

Figure 9. Absorption spectral change of SNP$_{60}$-poly(St-*co*-DE)-*block*-poly(NIPAm) (m = 137) in THF (a) and water (b) upon alternating irradiation with 313 nm light and visible light: open-ring form (broken line) and the photostationary state upon irradiation with 313 nm light (solid line).

Figure 10. Time-dependent change of the number of SNP$_{60}$-poly(St-*co*-DE) (M_n = 17000) (a) and SNP$_{60}$-poly(St-*co*-DE)-*block*-poly(NIPAm) (m = 137) (b) dispersed in THF and water. The sedimentation behavior was observed in the photostationary state.

Figure 11. Time-dependent change of number of (a) SNP$_{60}$-poly(St-*co*-DE)-*block*-poly(NIPAm) (m = 137) and (b) SNP$_{60}$-poly(St-*co*-DE)-*block*-poly(NIPAm) (m = 217) dispersed in water.

Figure 12. Time-dependent change of the number of SNP$_{60}$-poly(St-*co*-DE)-*block*-poly(NIPAm) (m = 137) dispersed in water at 25 °C (●) and 40 °C (○).

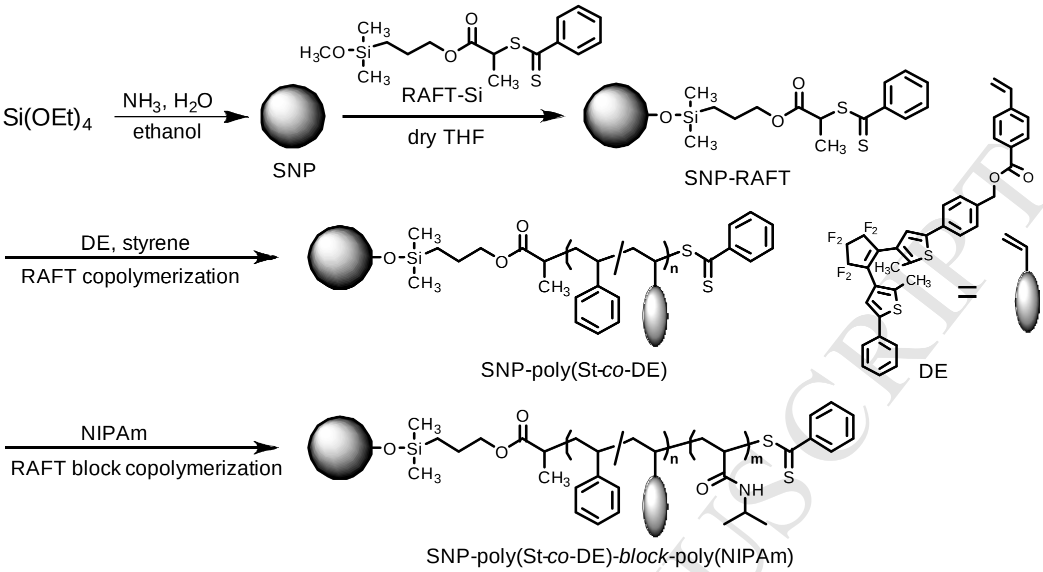

Scheme 1. Synthetic scheme of an amphiphilic photochromic silica nanoparticle.

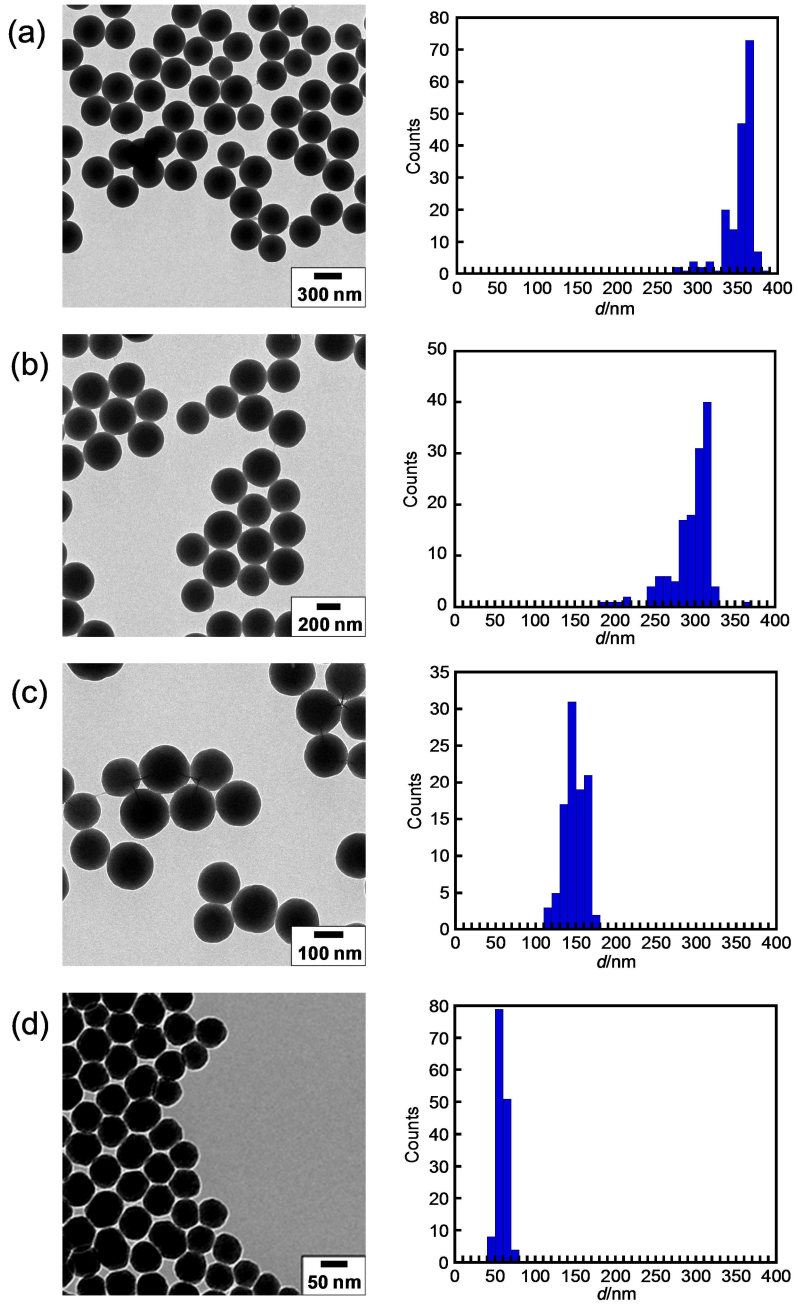

Figure 1. TEM images (left) and histograms of diameter distribution (right) for silica nanoparticles prepared by the Stöber method: [TEOS] = 0.11 mol L^{-1}, [NH_3] = 2.0 (a), 1.3 (b), 1.0 (c), 0.77 mol L^{-1} (d), [H_2O] = 2.4×[NH_3].

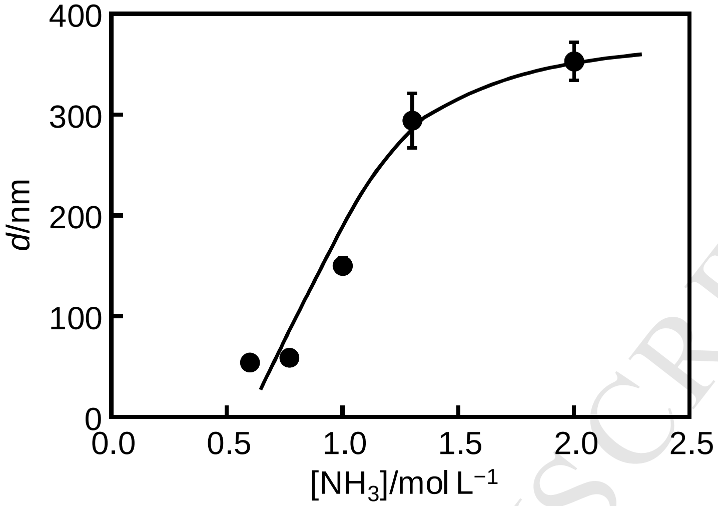

Figure 2. Relationship between the particle diameter of the silica nanoparticle and the concentration of ammonia used for the reaction. An error bar expresses the standard deviation of the particle diameter.

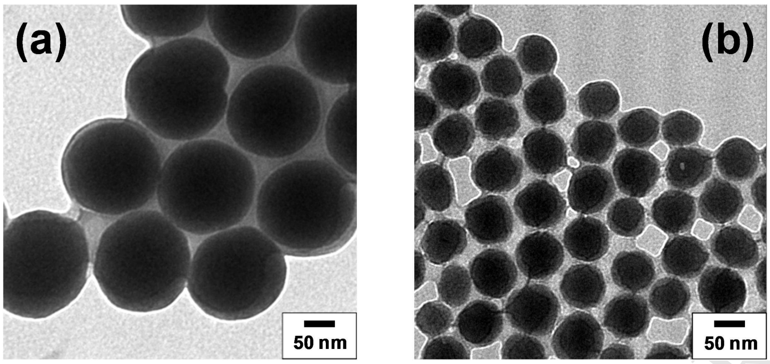

Figure 3. TEM images of SNP_{150}-poly(St-*co*-DE) (d = 150 nm, M_n = 27500) (a) and SNP_{60}-poly(St-*co*-DE) (d = 60 nm, M_n = 29800) (b).

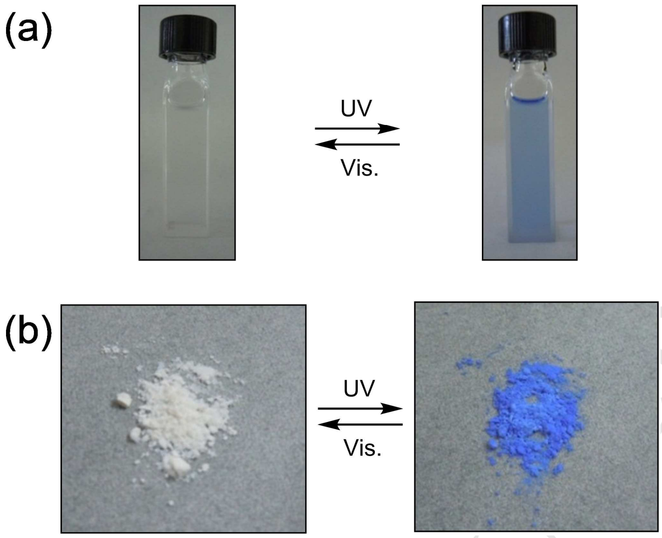

Figure 4. Photographs of SNP$_{60}$-poly(St-*co*-DE) (M_n = 29800) before (left) and after (right) irradiation with UV light in THF (a) and neat powder (b).

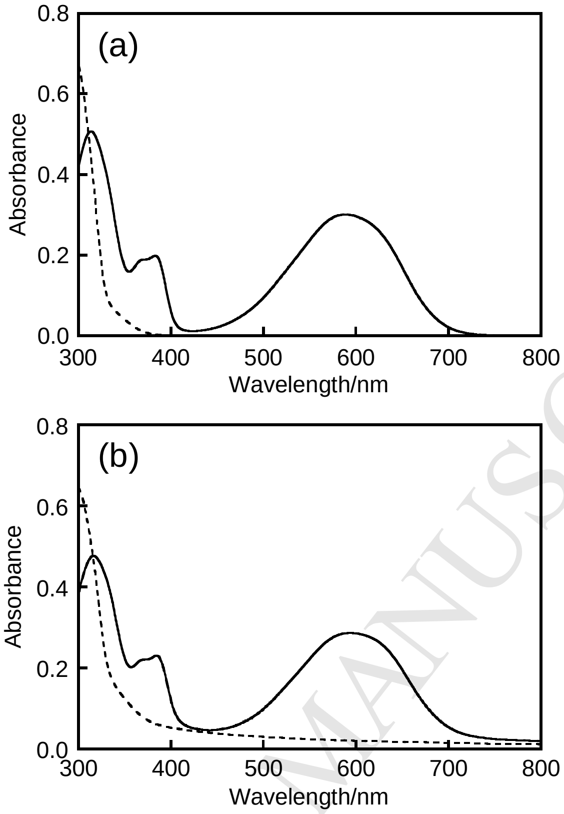

Figure 5. Absorption spectral changes of poly(St-*co*-DE) (a) and SNP$_{60}$-poly(St-*co*-DE) (M_n = 29800) (b) in THF: open-ring form (- - -) and the photostationary state upon irradiation with 313 nm light (——).

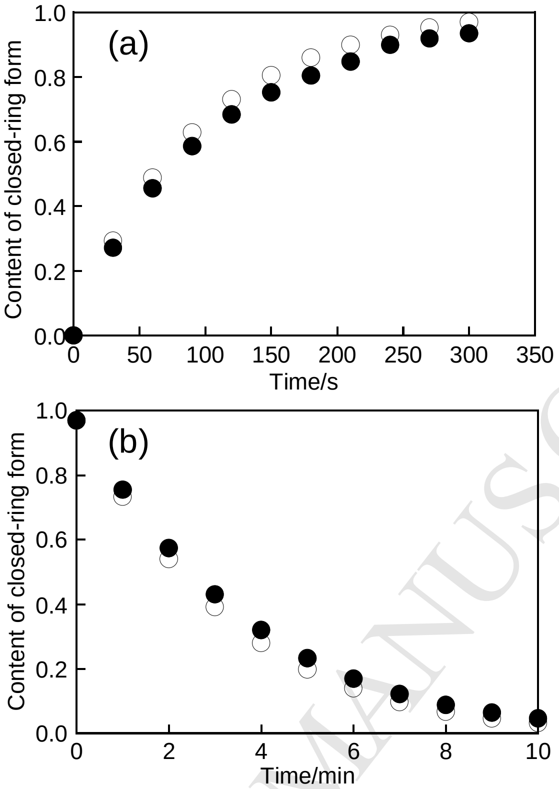

Figure 6. Time-conversion plot of SNP$_{60}$-poly(St-*co*-DE) (M_n = 29800) (●) and poly(St-*co*-DE) (○) in photocyclization by irradiation with 313 nm light (a) and in photocycloreversion by irradiation with 600 nm light (b).

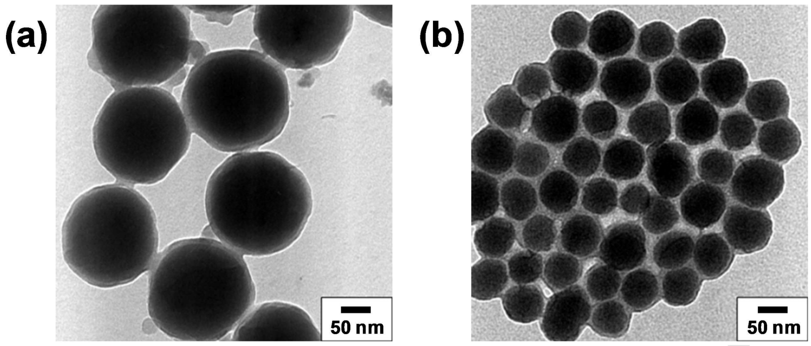

Figure 7. TEM images of SNP_{150}-poly(St-*co*-DE)-*block*-poly(NIPAm) (m = 160) (a) and SNP_{60}-poly(St-*co*-DE)-*block*-poly(NIPAm) (m = 137) (b).

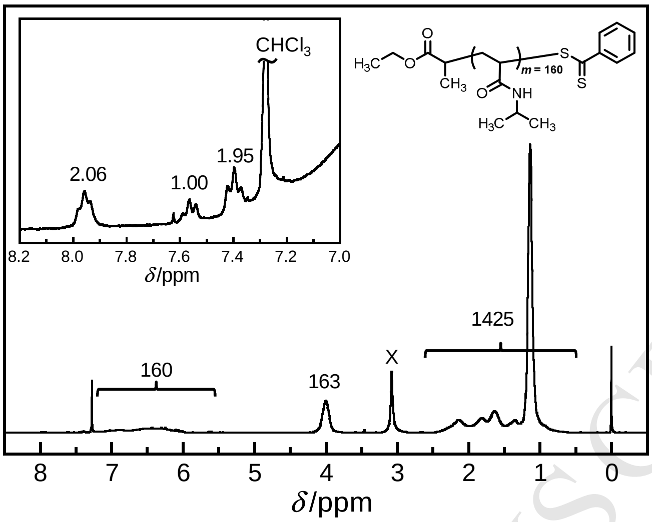

Figure 8. ^{1}H NMR spectrum of silica-free poly(NIPAm) obtained by RAFT polymerization of NIPAm with SNP$_{150}$-poly(St-*co*-DE) in DMF for 20 h at 60 °C: [NIPAm] = 3.5 mol L^{-1}, [EEDB] = 16 mmol L^{-1}, [SNP$_{150}$-poly(St-*co*-DE)] = 10 g L^{-1}, [AIBN] = 8.0 mmol L^{-1}.

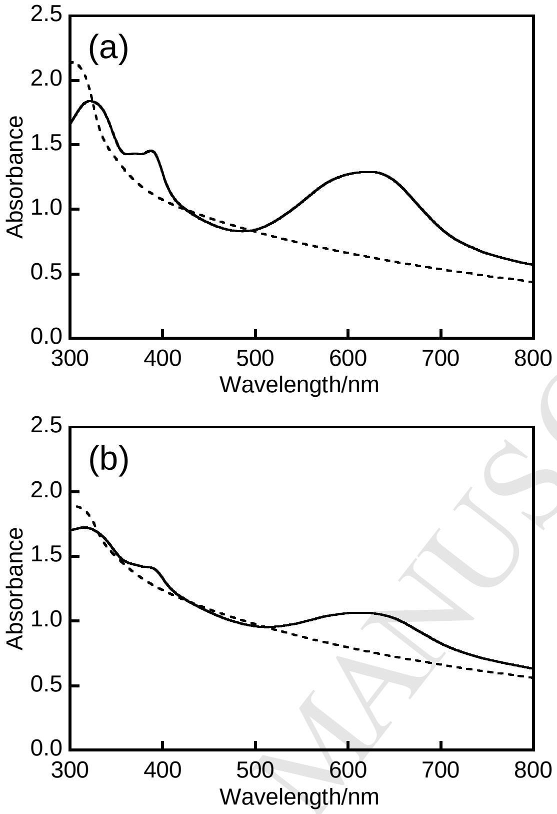

Figure 9. Absorption spectral change of SNP_{60}-poly(St-*co*-DE)-*block*-poly(NIPAm) (*m* = 137) in THF (a) and water (b) upon alternating irradiation with 313 nm light and visible light: open-ring form (broken line) and the photostationary state upon irradiation with 313 nm light (solid line).

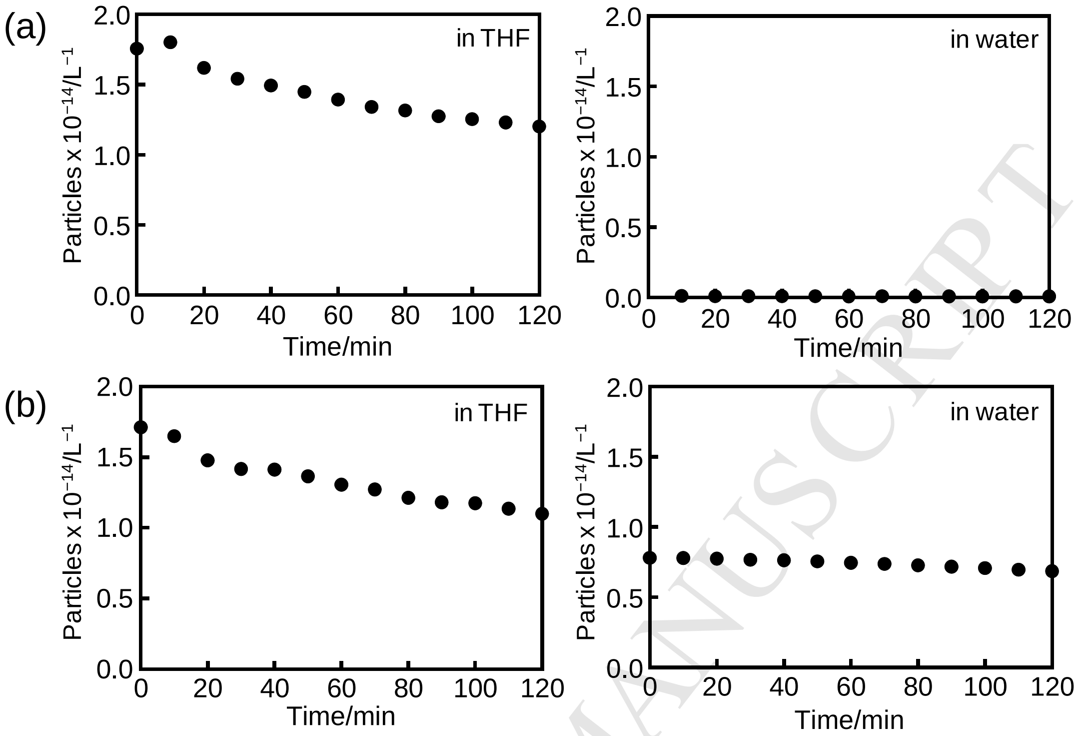

Figure 10. Time-dependent change of the number of SNP$_{60}$-poly(St-*co*-DE) (M_n = 17000) (a) and SNP$_{60}$-poly(St-*co*-DE)-*block*-poly(NIPAm) (m = 137) (b) dispersed in THF and water. The sedimentation behavior was observed in the photostationary state.

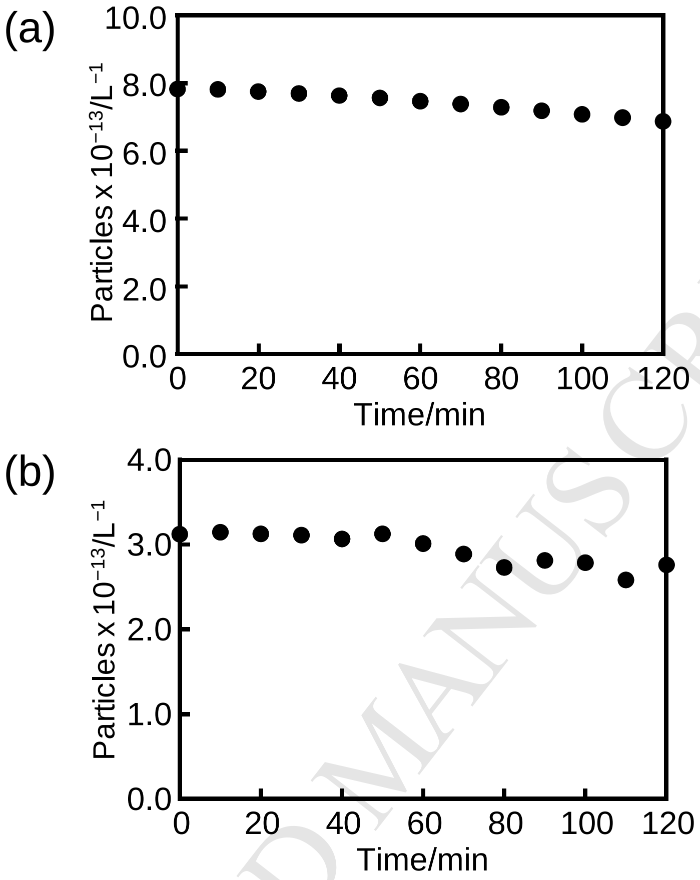

Figure 11. Time-dependent change of number of (a) SNP_{60}-poly(St-*co*-DE)-*block*-poly(NIPAm) (*m* = 137) and (b) SNP_{60}-poly(St-*co*-DE)-*block*-poly(NIPAm) (*m* = 217) dispersed in water.

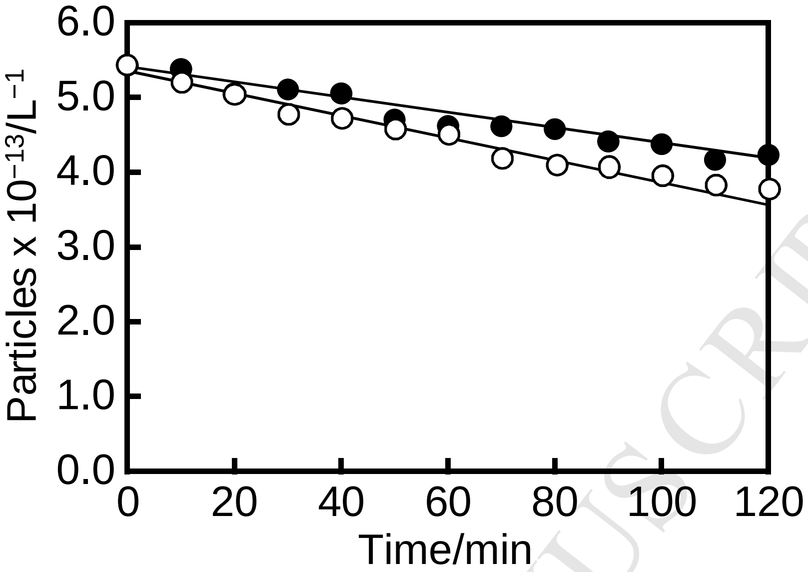

Figure 12. Time-dependent change of the number of SNP$_{60}$-poly(St-*co*-DE)-*block*-poly(NIPAm) (m = 137) dispersed in water at 25 °C (●) and 40 °C (○).

Table 1. Preparation conditions, average diameter (*d*), and standard deviation (σ) of silica nanoparticles prepared by the Stöber method in absolute ethanol for 24 h at r.t.

[TEOS] /mol L^{-1}	[NH_3] /mol L^{-1}	[H_2O] /mol L^{-1}	*d*/nm	σ/nm	(σ/*d*)/%
0.11	2.0	4.8	350	19	5.4
0.11	1.3	3.2	290	27	9.3
0.11	1.0	2.3	150	7.6	5.1
0.11	0.77	1.9	60	5.7	9.7
0.11	0.60	1.4	54	6.8	13

Table 2. RAFT copolymerization of St and DE in the presence of SNP-RAFT at 100 °C in toluene.[a)]

d [b)]/nm	σ [b)]/nm	[SNP-RAFT] /g L^{-1}	Time/h	Conversion[c)]/%	M_n [d)] (GPC)	M_w/M_n [d)] (GPC)	Molar fraction of DE[d)]/mol%
150[e)]	7.6	133	9	36.3	27500	1.15	39
60[e)]	5.7	133	18	43.3	29800	1.20	37
60[e)]	5.7	80	20	37.3	17000	1.20	34
60[e)]	5.7	50	20	43.3	24200	1.19	34

a) [St] = 2.25 mol L^{-1}, [DE] = 0.75 mol L^{-1}, [EEDB] = 5.0 mmol L^{-1}, [ATMP] = 0.50 mmol L^{-1}.

b) Diameter (*d*) and standard deviation (σ) of SNP.

c) Percentage of monomers used to form SNP-poly(St-*co*-DE) or poly(St-*co*-DE).

d) Number average molecular weight, polydispersity, and molar fraction of DE of silica-free poly(St-*co*-DE) obtained by RAFT copolymerization of St and DE in the presence of SNP-RAFT.

e) The resulting silica nanoparticles (*d* = 150 and 60 nm) covered with the polymers are called SNP_{150}-poly(St-*co*-DE) and SNP_{60}-poly(St-*co*-DE), respectively.

Table 3. RAFT block copolymerization of NIPAm using SNP-poly(St-*co*-DE) in DMF at 60 °C: [NIPAm] = 3.5 mol L^{-1}, [EEDB] = 16 mmol L^{-1}, [SNP-poly(St-*co*-DE)] = 10 g L^{-1}, [AIBN] = 8.0 mmol L^{-1}

SNP-poly(St-*co*-DE)		Time/h	Conversion/%	m [c]
d [a]/nm	M_n [b]			
150	27500	20	59.2	160
60	17000	20	50.5	137
60	24200	40	66.5	217

a) Diameter of SNP in SNP-poly(St-*co*-DE).

b) M_n of silica-free poly(St-*co*-DE).

c) Degree of polymerization for poly(NIPAm) obtained in the RAFT polymerization.

Graphical Abstract

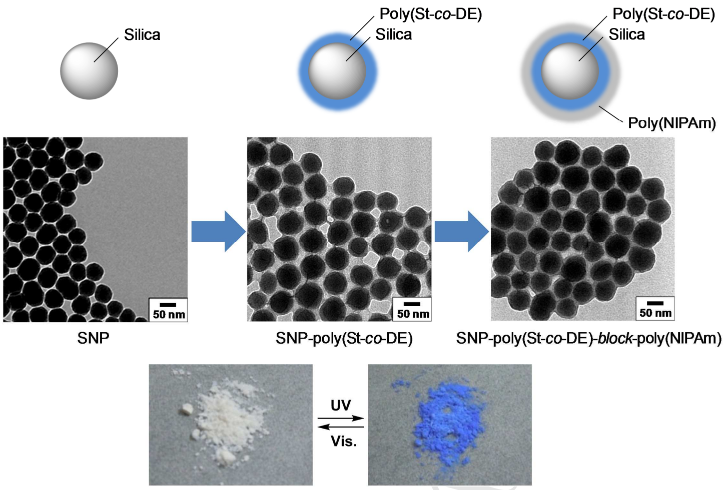

Highlights:

We succeeded in preparing organic/inorganic hybrid photochromic pigments.

The photochromic block copolymers are grafted on silica nanoparticle.

The block copolymers were prepared by a living radical polymerization.

The organic/inorganic hybrid pigments are well-dispersed in tetrahydrofuran and water.

The organic/inorganic hybrid pigments show photochromism in solution and powder.